ELEMENT-WISE EQUALIZATION OF LINE ARRAYS

Lukas Gölles[1], Matthias Frank[1], Franz Zotter[1]

[1] *Institute of Electronic Music and Acoustics, University of Music and Performing Arts, Graz, Austria*

This paper is a revised version of the authors' submitted manuscript that was peer-reviewed by at least two anonymous reviewers.

Preliminary document

Abstract

Curved line arrays are typically optimized through geometric curvature and, when needed, delay loading to realize a prescribed direct-sound level decay over distance. While this effectively controls broadband level distribution, spectral inconsistencies remain due to discretization, element-to-element variability, and mutual coupling. This work proposes an element-wise equalization method that is directly linked to the curvature design via stationary-phase observation points. For each enclosure, distance- and frequency-dependent responses are measured at its associated observation point, third-octave-averaged, and converted to a minimum-phase representation using real-cepstrum processing with cepstral windowing. Band-limited spectral inversion then yields a per-enclosure equalizer, with RMS normalization preserving the intended decay profile. Concert-hall measurements on a six-element RCF HDL26-A array demonstrate reduced spectral spread compared with a single common equalizer, particularly above 1 kHz. The approach improves frequency consistency while maintaining the desired A-weighted direct-sound attenuation, providing a practical complement to geometry-driven array design.

Keywords: *sound reinforcement, line array, filter design*

1. Introduction

Line arrays are central to modern sound reinforcement for shaping directivity and controlling level decay over large audiences. A line source can be curved and/or delay-loaded to realize a desired direct sound pressure level roll-off over the listening area. The Wavefront Sculpture Technology (WST) criteria by Heil and Urban formalize coupling, curvature, and phase alignment to approximate continuous behavior with discrete elements [1, 2]. Practice-oriented treatments detail how splay, spacing, and tuning affect uniformity and interference [3–5]. Array-theoretic work (Dolph–Chebyshev, Taylor) clarifies tapering trade-offs between mainlobe width and sidelobes [6–8], and constant-beamwidth transducers (CBTs) underscore the role of non-flat apertures in stabilizing coverage [9, 10].

Building on these principles, recent analytical and numerical studies of curved/phased line sources provide control laws for direct-sound decay and coverage, with implementations for immersive reinforcement [11–14]. Curvatures derived from differential equations can enforce target attenuation while steering stationary-phase directions that dominate the perceived sound pressure level. The stationary-phase viewpoint, widely used in sound field synthesis and spatial audio [15, 16], links local source inclination to representative audience-plane observations.

In practice, arrays are discrete, finite, and subject to element variability and mutual coupling, introducing frequency-dependent artifacts: (i) spatial aliasing from finite spacing, (ii) truncation and sidelobes, and (iii) position-dependent comb filtering, especially near the array. Thus, spatially uniform broadband level control does not guarantee spectral uniformity; variability often persists even when decay targets are met [3, 11, 14].

A common mitigation is a single global equalizer from spatial averages, which reduces broad trends but underfits location-specific deviations and can mask near-field interference. Alternatively, element-wise equalization applies enclosure-specific amplitude and minimum-phase corrections to improve local spectral balance while preserving the global decay set by geometry. Minimum-phase EQ offers latency-efficient, stable compensation; real-cepstrum analysis with cepstral windowing separates minimum- and excess-phase terms. Band-limited inversion restricts EQ to the reliable passband, established via fractional-octave analysis and robust measurements [17, 18].

We propose an element-wise equalization framework tied to curvature design via stationary-phase observation points—audience-plane locations representative for each enclosure's contribution. The method integrates: (i) geometry-anchored per-enclosure observation points, (ii) third-octave averaging to stabilize spec-

Corresponding author: *goelles@iem.at.*

Copyright: *©2026 Gölles et al. This is an open-access article distributed under the terms of the Creative Commons Attribution 3.0 Unported License, which permits unrestricted use, distribution, and reproduction in any medium, provided the original author and source are credited.*

tra under small-scale interference, (iii) real-cepstrum processing with cepstral windowing for minimum-phase targets, and (iv) band-limited inversion with RMS normalization to preserve the intended decay [11, 13, 14]. We evaluate a six-element RCF HDL26-A array in a concert hall against a conventional common EQ. Results show a marked reduction in spectral spread—particularly above 1 kHz and near the array where comb filtering is strongest—while maintaining the target attenuation profile set by the curvature.

2. Design of Line Array Curvature

Within a multi-target design approach by combining curving and phasing of line sources, recent research introduces a nonlinear differential equation of the local inclination ϑ [11] that defines the curvature and phasing of a line array in order to achieve a direct-sound attenuation of $-6{\cdot}\beta$ dB per doubling of distance. Here, we focus only on curved sources. Therefore, the phasing term introduced in [11] is omitted. The curvature $\dot{\vartheta}$ as derivation of the local inclination ϑ over the natural length parameter s is then given by

$$\dot{\vartheta} = -\frac{r^{2\beta}}{g^2}\frac{1}{r^2} + \frac{1}{r} \qquad \text{with } r = \frac{z}{\sin\vartheta}\,. \tag{1}$$

Here, g denotes a gain parameter and r represents the distance at which the time of flight to the source is minimal for a receiver $\boldsymbol{x}_\mathrm{r}$ located in the x-y plane. The resulting convex array geometry is obtained by integration along the natural length parameter s,

$$\boldsymbol{x} = \int \boldsymbol{t}\,\mathrm{d}s + \boldsymbol{x}_0\,, \qquad \boldsymbol{t} = \begin{bmatrix}\sin\vartheta & 0 & \cos\vartheta\end{bmatrix}^\intercal\,. \tag{2}$$

The algorithm presented in [11, Alg. 2] provides a numerical solution of Equations (1) and (2) for a continuous source design, which is subsequently discretized.

3. Overview of the procedure

First, the differential equation is solved and discretized. For a discrete source a web-based JavaScript solver.[1] already proposes tilt angles and the corresponding observation point for each line-array enclosure. Each measurement point is chosen along the local on-axis (stationary-phase) direction, i.e., the direction that minimizes the time of flight for a receiver in the audience plane.

At any point on the source, we define the on-axis stationary-phase direction

$$\boldsymbol{u} = \begin{bmatrix}\cos\vartheta & 0 & -\sin\vartheta\end{bmatrix}^\intercal\,, \tag{3}$$

which is the unit normal vector to the local tangent direction $\boldsymbol{t}$ of the curved source, determined by the local inclination ϑ of the curved source. The intersection of this direction with the listening plane yields the observation point associated with that source location (i.e., the stationary-phase observation point),

$$\boldsymbol{x}_\mathrm{r} = \boldsymbol{x} + \frac{z}{\sin\vartheta}\begin{bmatrix}\cos\vartheta & 0 & -\sin\vartheta\end{bmatrix}^\intercal\,, \tag{4}$$

where $\boldsymbol{x} = [x,\,y,\,z]^\intercal$ denotes the source point in a global coordinate system.

At each of these observation points $\boldsymbol{x}_\mathrm{r}$, impulse response measurements $h[\boldsymbol{x}_\mathrm{r}, n]$ are taken. The corresponding magnitude responses are computed and averaged in third-octave bands, yielding $|H[\boldsymbol{x}_\mathrm{r}, k]| = |\mathcal{F}\{h[\boldsymbol{x}_\mathrm{r}, n]\}|$, where $\mathcal{F}\{\cdot\}$ denotes the discrete Fourier transform (DFT).

To analyze the distance- and frequency-dependent sound pressure, the real cepstrum is computed as

$$C_\mathrm{r}[\boldsymbol{x}_\mathrm{r}, m] = \Re\left\{\mathcal{F}^{-1}\big(\log(|H[\boldsymbol{x}_\mathrm{r}, k]|)\big)\right\}, \tag{5}$$

where $|\cdot|$ is the elementwise magnitude, $\log(\cdot)$ the elementwise natural logarithm, m the quefrency index and $\Re\{\cdot\}$ denotes the real part.

We use the standard homomorphic (real-cepstrum) method to derive a minimum-phase target based on the theory of homomorphic signal processing [19]. This procedure is equivalent to widely used implementations such as MATLAB's `rceps`[2] and SciPy's `minimum_phase`[3]. We insert a third-octave smoothing step prior to the log magnitude to stabilize the magnitude estimate.

To obtain a minimum-phase filter, we apply a standard cepstral window $w[\tau]$ to $C_\mathrm{r}[\boldsymbol{x}_\mathrm{r}, \tau]$:

$$w[m] = \begin{cases} 1, & m = 0 \text{ or (if } N \text{ even) } m = \dfrac{N}{2}, \\ 2, & 1 \le m \le \left\lfloor \dfrac{N}{2} \right\rfloor - 1, \\ 0, & \text{otherwise,} \end{cases} \tag{6}$$

where N is the length (in quefrency samples) of $C_\mathrm{r}[\boldsymbol{x}_\mathrm{r}, m]$. The minimum-phase impulse response is then given by

$$h_{\text{min.phase}}[\boldsymbol{x}_\mathrm{r}, n] = \Re\left\{\mathcal{F}^{-1}\Big(\exp\Big(\mathcal{F}\{\,w[m]\cdot C_\mathrm{r}[\boldsymbol{x}_\mathrm{r}, m]\}\Big)\Big)\right\}, \tag{7}$$

where $\exp(\cdot)$ is elementwise exponentiation, and $\mathcal{F}^{-1}\{\cdot\}$ is the inverse DFT and the multiplication is elementwise.

The equalization filter is obtained by inverting the frequency response of $h[\boldsymbol{x}_\mathrm{r}, n]$:

$$h_\mathrm{EQ}[\boldsymbol{x}_\mathrm{r}, n] = \Re\left\{\mathcal{F}^{-1}\left(\frac{1}{\mathcal{F}\{h_{\text{min. phase}}[\boldsymbol{x}_\mathrm{r}, n]\}}\right)\right\}, \tag{8}$$

where the division is elementwise.

To avoid unnatural amplification at the spectral ex-

[1] https://enimso.iem.sh/post/line-array-designer-with-spl-estimation/

[2] https://uk.mathworks.com/help/signal/ref/rceps.html?s_tid=srchtitle_support_results_1_rceps

[3] https://docs.scipy.org/doc/scipy/reference/generated/scipy.signal.minimum_phase.html

Preliminary document

tremes, $h_{\mathrm{EQ}}[\boldsymbol{x}_{\mathrm{r}}, n]$ is further shaped by appropriate high-pass and low-pass filters. This constrains the equalization to the effective passband of the loudspeaker, accounting for its finite low-frequency extension and high-frequency roll-off.
Finally, the equalization impulse responses $h_{\mathrm{EQ}}[\boldsymbol{x}_{\mathrm{r}}, n]$ are normalized to a common RMS level to preserve the intended direct-sound level decay established by the array curvature. The resulting per-enclosure filters are then used for equalization of the corresponding line-array elements.

Choice of minimum-phase filters.
We use minimum-phase FIR targets to minimize added latency, which is critical for live reinforcement and for preserving temporal alignment between the array and stage acoustics. Minimum-phase EQ inevitably alters the mechanical/geometry-induced phase alignment of the line-array elements; however, the resulting group delays are small compared to the time-of-flight differences set by curvature and audience distance, and we found no adverse artifacts in the measured results. If some latency is acceptable, linear-phase FIR can better preserve the enclosure-to-enclosure phase relationships while providing symmetric pre/post-ring control at high frequencies. Exploring such latency-controlled, linear/hybrid-phase designs is promising future work. Here we focus on the minimum-latency solution.

4. Measurements of an RCF HDL26-A line array

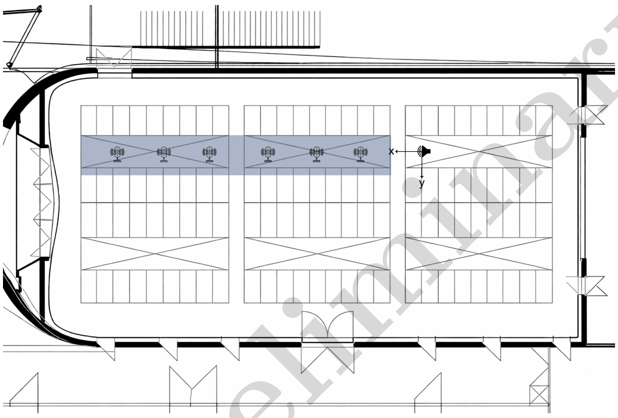

Figure 1: Top view: Loudspeaker and microphone positions in György-Ligeti Hall of the University of Music and Performing Arts Graz, and desired coverage distance (light blue). The x–y coordinate axes are shown; z points upward.

We assume a sound reinforcement scenario in the György-Ligeti Hall of the University of Music and Performing Arts Graz, a concert hall with dimensions 32 m × 16 m and a reverberation time of $T_{60} \approx 1.3\,\mathrm{s}$. The source is mounted at a distance of 9 m from the rear wall, assuming a stage in front (cf. Figure 1). The origin is chosen to be below the source, and the listening area is assumed to lie on the x–y plane. The area to be covered by the line source starts at $x_{\mathrm{r}} = 2\,\mathrm{m}$ and extends to $x_{\mathrm{r}} = 22\,\mathrm{m}$. We use six RCF HDL26-A line-array elements in the chain. The flybar is rigged at a height of 3 m above the listening area, establishing the suspension point for the array.
Our goal is to design the array for immersive sound reinforcement of classical and pop concerts. Therefore, we choose a slightly relaxed level decay of −1 dB per doubling of distance (dod.), which provides a good compromise between balanced direct-sound levels of objects, preservation of envelopment, and improved frequency consistency over distance [20]. The differential equation (1) proposes the curvature of the continuous source, which is then discretized to form a source with six discrete enclosures. The web-based line-array solver proposes the tilt angles and also the measurement positions along the on-axis direction[4],

$$x_{\mathrm{r}} \in \{4,\ 6,\ 10,\ 14,\ 17,\ 20\}\,\mathrm{m}.$$

For the measurements, an NTI measurement microphone was positioned at ear height for a standing audience, i.e., 1.5 m.
Figure 4 shows the frequency responses for a set of observation points without applying any processing to the array. We truncated the impulse response at 50 ms to isolate the direct sound and early arrivals from the subsequent reverberation. In this and all subsequent frequency-response plots, we normalize each response within the band 1 kHz–3 kHz to facilitate comparison of spectral shapes rather than the direct sound pressure level decay settings of the line array.
The frequency response reveals that lower frequencies are more pronounced than higher frequencies, which is a typical line-array behavior when stacking multiple loudspeakers with rather uniform magnitude response as shown in Figure 2 that displays the on-axis frequency response of a single RCF line-array enclosure. In [11], it was shown that line sources composed of ideal point sources exhibit a 3 dB/octave rise toward lower frequencies.
Figure 3 shows the magnitude response of the filters resulting from the proposed algorithm. When these filters are applied to the individual line-array enclosures, the frequency responses in Figure 5 are obtained. Compared to the unprocessed responses, the equalization clearly corrects the spectral imbalance. Furthermore, from around 1 kHz upward, the responses align very closely. Above 8 kHz, small deviations can still be observed.
At this point, it is instructive to compare the proposed procedure with a conventional approach. Typically, the array would be mounted, measurements would be taken on site, and a single equalizer would be designed for the entire array. For this conventional equalizer, the frequency responses at the measurement positions are RMS-averaged, and the filter design procedure using the cepstrum, as described in section 3 is applied

[4] `https://enimso.iem.sh/post/line-array-designer-with-spl-estimation/?N=6&h=0.223&z0=3&xr0=22&xrS=2&beta=0.1&b=0`

Preliminary document

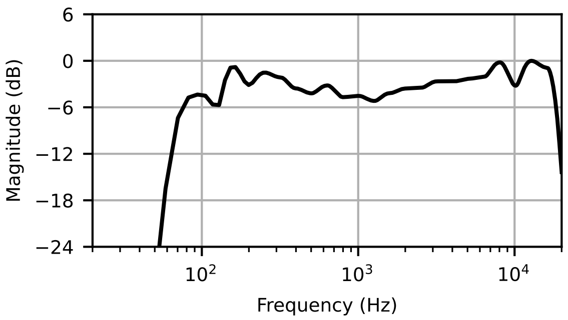

Figure 2: Third-octave-averaged on-axis frequency response of a Mini Line Array element from [21].

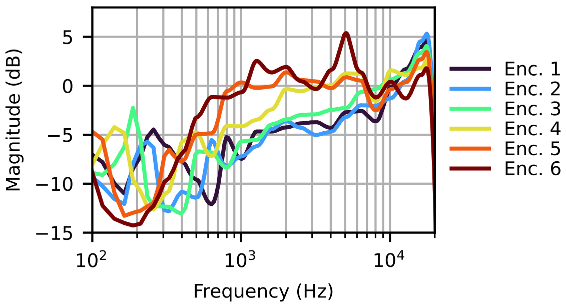

Figure 3: Equalization filters for each enclosure of the RCF line array (individual EQ).

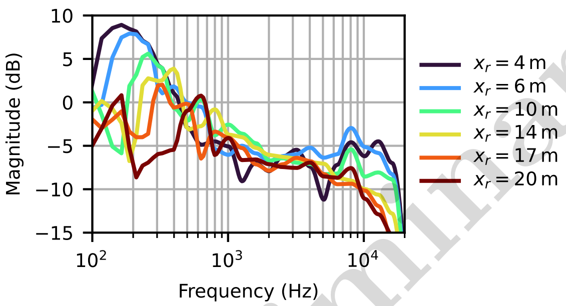

Figure 4: Third-octave-averaged on-axis frequency responses of a six-element line array at several observation points before equalization (each normalized between 1 kHz and 3 kHz).

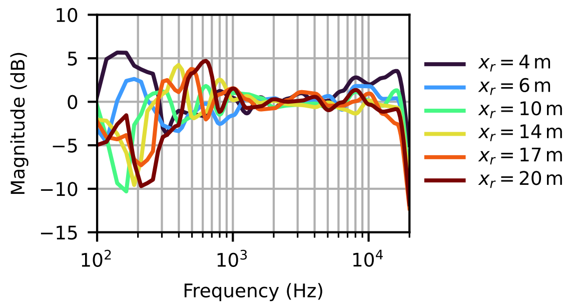

Figure 5: Third-octave-averaged on-axis frequency responses with applied per-enclosure equalization using the proposed algorithm (each normalized between 1 kHz and 3 kHz).

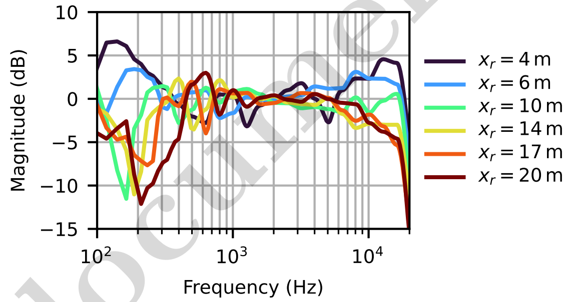

Figure 6: Third-octave-averaged on-axis frequency responses with a single common equalization filter applied to all enclosures (each normalized between 1 kHz and 3 kHz).

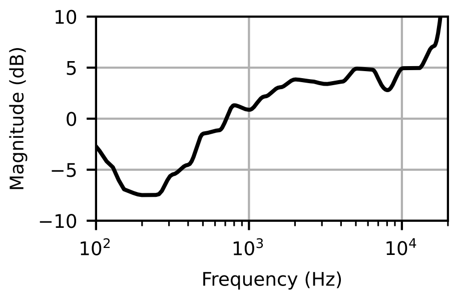

Figure 7: Frequency response of the common equalization filter applied to the entire array.

Preliminary document

to this averaged response. Applying this common filter to all enclosures results in the magnitude responses shown in Figure 6. The differences between the proposed procedure (individual filters per enclosure) and the conventional overall filter are especially evident above 1 kHz. While the common-filter approach yields good results in that range, individual filters reduce the differences. Still at very high frequencies above 8 kHz, a smaller spread between the responses remains noticeable when using individual filters.

For the closest observation point at $x_\mathrm{r} = 4\,\mathrm{m}$, the comb-filter structure visible in Figure 6 is largely mitigated in Figure 5. The high-frequency response at near observation points is also improved by using individual filters.

To compare the results of both methods quantitatively, Figure 8 and Figure 9 show the RMS average over all responses for both approaches as well as the spread between minimum and maximum values (shaded area). As already seen, at higher frequencies the individual-filter approach outperforms the common-filter method. Figure 10 compares the spread (difference between minimum and maximum level) for both methods, underlining the advantage of using individual filters above 1 kHz. The median spread across $1-10$kHz drops from 2.99 dB (common EQ) to 1.62 dB (individual EQ). Below 1 kHz, no substantial improvements are expected, as the line-source radiation becomes effectively point-source-like for frequencies below approximately 750 Hz at observation points beyond $x_\mathrm{r} = 4\,\mathrm{m}$, i.e.,

$$f = \frac{c}{r_b\, L^2}, \tag{9}$$

where $L = 6 \cdot 0.22$m denotes the length of the line array, r_b the transition radius between near and far field and $c = 343\,\mathrm{m\,s^{-1}}$ the speed of sound [22].
Across the entire distance range (3 m - 20 m), the A-weighted levels for the three conditions (individual EQ, common EQ, no EQ) track each other closely. The inter-condition spread is small—typically $<$ 1 dB(A)—indicating that the choice of EQ has only a minor influence compared with the distance-dependent trend, cf. Figure 11.

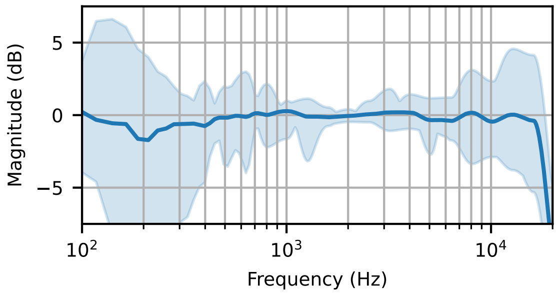

Figure 8: RMS-averaged response (solid) across all observation points with shaded spread (min–max) for the common-filter approach.

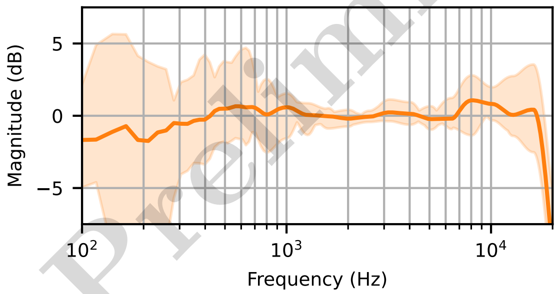

Figure 9: RMS-averaged response (solid) across all observation points with shaded spread (min–max) for the individual-filter approach.

In [23], we provide listening examples. For these, we measured first-order Ambisonic room impulse responses (RIRs) and upmixed them to fifth order using the SD-ASDM approach [24]. The resulting impulse responses are convolved with the EBU male speech reference [25] and with an excerpt of "What's Trumps"

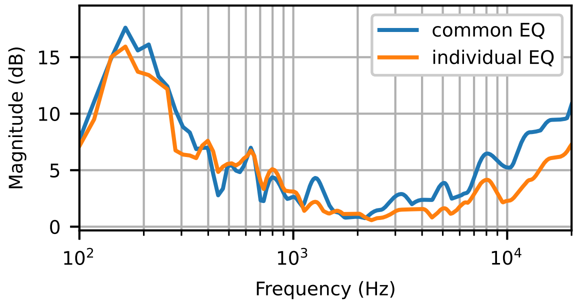

Figure 10: Comparison of the spread (difference between minimum and maximum levels) for both approaches: common versus individual EQ.

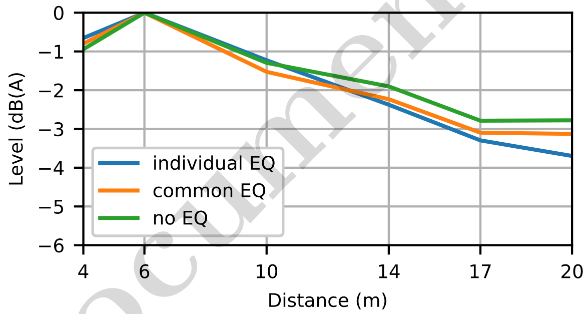

Figure 11: Comparison of the A-weighted sound pressure levels over distance.

performed by Rhythmussportgruppe [26].

5. Conclusion

We presented an element-wise equalization strategy for curved line arrays that is tightly coupled to the geometric design via stationary-phase observation points. For each enclosure, a minimum-phase target is obtained from third-octave-averaged measurements using real-cepstrum processing, and a band-limited spectral inversion yields per-enclosure FIR filters. RMS normalization ensures that the equalization preserves the intended A-weighted decay established by the array curvature.
Simulations and measurements with a six-element RCF HDL26-A array showed that the proposed method reduces spectral variability relative to a single common equalizer, in particular above 1 kHz.
Further research should be done in extending the method to analytical calculation of the equalization filters by using the magnitude response of the .GLL files - typically used in EASE. Furthermore, an automatic proposal of IIR parameters that can be used directly by the DSP of the RCF enclosures would improve the system setup in practice.

6. Acknowledgment

The RCF line arrays are funded by the (digital) research infrastructure project "Interactive audiovisual

Preliminary document

digital twins of performance venues" by the Austrian Federal Ministry of Women, Science and Research.

7. Data Availability

To support reproducible research, the omni directional impulse responses of each line array enclosure as well as listening examples are made available under [23].

References

[1] C. Heil and M. Urban, "Sound fields radiated by multiple sound sources arrays," in *92nd AES Convention*, Vienna, Austria, 1992.

[2] M. Urban, C. Heil, and P. Bauman, "Wavefront sculpture technology," *J. Audio Eng. Soc*, vol. 51, no. 10, pp. 912–932, 2003.

[3] B. McCarthy, *Sound Systems: Design and Optimization*, 3rd ed. Oxford, UK: Focal Press, 2016.

[4] D. Davis and E. Patronis, *Sound System Engineering*, 4th ed. New York, USA: Routledge, 2013.

[5] M. S. Ureda, "Line Arrays: Theory and Applications," in *110th AES Convention*, AES, Amsterdam, The Netherlands, 2001.

[6] C. L. Dolph, "A current distribution for broadside arrays which optimizes the relationship between beam width and side-lobe level," *Proceedings of the IRE*, vol. 34, no. 6, pp. 335–348, 1946.

[7] T. T. Taylor, "Design of line-source antennas for narrow beamwidth and low side lobes," *Transactions of the IRE Professional Group on Antennas and Propagation*, vol. AP-3, no. 1, pp. 16–28, 1955.

[8] R. C. Hansen, *Phased Array Antennas*, 2nd ed. Hoboken, USA: Wiley, 2009.

[9] J. D. B. Keele, "The application of constant-beamwidth transducer (cbt) line arrays to sound reinforcement," in *109th AES Convention*, Los Angeles, USA, 2000.

[10] J. D. B. Keele, "What's so sacred about exponential horns? constant-beamwidth transducers," *Journal of the Audio Engineering Society*, vol. 51, no. 5, pp. 512–539, 2003.

[11] L. Gölles and F. Zotter, "Theory of continuously curved and phased line sources for sound reinforcement," *Acta Acust.*, vol. 7, p. 52, 2023.

[12] F Zotter and L. Gölles, "Curvature and delay-based line-array design," in *Fortschritte der Akustik (DAGA)*, Hannover, Germany, Mar. 2024.

[13] L. Merkel, F. Zotter, and L. Gölles, "Simulating the direct-sound coverage from the directivity measurement of a fully assembled mini line array," in *Fortschritte der Akustik (DAGA)*, Hannover, Germany, Mar. 2024.

[14] L. Gölles and F. Zotter, "Dual-Target Design for Large-Scale Sound Reinforcement: Simulation and Evaluation," in *AES Conference: AES 2024 International Acoustics & Sound Reinforcement Conference*, AES, Le Mans, France, 2024.

[15] S. Spors and J. Ahrens, "Analytical driving functions for higher-order ambisonics and wave field synthesis using the stationary phase approximation," in *124th AES Convention*, Amsterdam, The Netherlands, 2008.

[16] J. Ahrens, *Analytic Methods of Sound Field Synthesis*. Berlin, Germany: Springer, 2012.

[17] *IEC 61260: Electroacoustics – Octave-band and fractional-octave-band filters*, Consolidated version; verify part and edition as used, International Electrotechnical Commission, 2014.

[18] A. Farina, "Simultaneous Measurement of Impulse Response and Distortion with a Swept-Sine Technique," in *108th AES Convention*, AES, Paris, France, 2000.

[19] A. Oppenheim and R. Schafer, "Homomorphic analysis of speech," *IEEE Transactions on Audio and Electroacoustics*, vol. 16, no. 2, pp. 221–226, 1968.

[20] L. Gölles, M. Frank, and F. Zotter, "Evaluating a dual-target line-array design for medium-scale surround sound reinforcement," in *156th AES Convention*, Madrid, Spain, Jun. 2024.

[21] L. Gölles, F. Zotter, and L. Merkel, "Miniature line array for immersive sound reinforcement," in *Audio Engineering Society Conference: AES 2023 International Conference on Spatial and Immersive Audio*, 2023.

[22] L. Gölles and F. Zotter, "Approximating the direct sound pressure level of line sources," in *Fortschritte der Akustik (DAGA)*, Dresden, Germany, Mar. 2026.

[23] L. Gölles, *Supplementary Data for Element-wise Equalization of Line Arrays*, 2026. [Online]. Available: `https://phaidra.kug.ac.at/o:137221`.

[24] L. Gölles and M. Frank, "Ambisonic spatial decomposition method with salient / diffuse separation.," in *158th AES Convention*, Warsaw, May 2025.

[25] EBU, *EBU SQAM CD: Sound Quality Assessment Material recordings for subjective tests*, EBU SQAM CD: Sound Quality Assessment Material recordings for subjective tests, 2008.

[26] D. Leckschat, C. Epe, N. Dahlheimer, M. Bier, L. Prinz, and H. Schulte, *Tonproduktion zweier Titel des Funk-Ensembles "Rhythmussportgruppe"*, version 1.0, Feb. 2020.

Preliminary document